

Topology and Minimal Group Representation of the Classical Dual Sector of Quantum Theory

Diego J. CIRILO-LOMBARDO

*Instituto de Física Interdisciplinaria y Aplicada (INFINA)-Departamento de Física UBA,
CONICET, Buenos Aires C1428EGA, Argentina.*

*AGN (Active Galactic Nucleus) Group, Radio Astrophysics,
Special Astrophysical Observatory (SAO) - Russian Academy of Sciences and
Laboratory of Information Technologies (LIT) Joint Institute for Nuclear Research (JINR),
Dubna (Moscow Region) Russian Federation*

Norma G. SANCHEZ

*The International School and Institute of Astro-Physics Daniel Chalonge - Hector de Vega,
CNRS, INSU-Institut National des Sciences de l'Univers,
Sorbonne University, 75014 Paris France,*

Norma.Sanchez@obspm.fr, <https://chalonge-devega.fr/sanchez>

(Date textdate; Received textdate; Revised textdate; Accepted textdate; Published textdate)

Abstract

In this paper we compute and analyze the geometrical and topological changes in quantum physics within the new framework of our recent work [APL Quantum 2, 016104 (2025)] on Classicalization. Thus, the results of our paper here are twofold : **Topology, geometry and Classicalization and the relationship between them.** With this end, we consider various types of states on the simplest polygon: states with triangle topology as solution of the Schrodinger equation, eigenstates of a lowering operator and coset coherent states. The results of this paper are: **(1)** From the point of view of the metaplectic group and the classicalization, the application of the Minimal Group Representation (MGR) on the states on the triangle and the circle can be performed only if the ladder operators A_n and A_{-n} are related to those of the oscillator a and a^+ . **(2)** For the coherent state case, the application of the MGR can be viewed in the same way as (1) but considering an eigenstate of the operator A_{-1} , or a more general case, as an eigenstate of A_{-n} . **(3)** These 2D states are edge states geometrically dual to the quantum states within the boundary of the triangle: there is interplay between states at the edge and the states inside the triangular boundary. **(4)** The coherent states in the triangle are generated by applying the group D_3 to the coset coherent states of the circle as a fiducial vector (e.g., a polygon with infinity sides). **(5)** The justification for the proposal in item **(4)** is easy to see by applying the cyclic subgroup C_n of D_n to the fiducial (coset circle coherent states): as the number of sides tends to infinity, the elements of C_n tend to the identity. **(6)** The application of MGR in the case of D_3 (D_n) coherent state, reveals to us the quantum structure underlying each of the sides of the triangle (polygon). **(7)** The norm (probability) found shows a clear interaction/interference between the sides of the triangle and between the even and odd sectors of the Hilbert space. **(8)** The application of MGR allows topological isolation between the projected sectors (even and odd). It can be seen that the topological effect is of a quantum nature and vice versa. **(9)** These topological isolation effects do not disappear at the macroscopic level (e.g. they are independent of the space-time parameters of the physical system). In general, the results here show too that quantum states in geometries with angles and vertices classicalize more than in geometries without them. **(10)** Within this context, a generalization of the Bargmann representation, not previously introduced in the literature, is presented. **(11)** These theoretical results can have impact and applications in : Classical and quantum information processing, Quantum computation, classical-quantum interaction and interpretation measurements, classical-quantum duality, classical or quantum optimization.

Contents

I. Introduction and Results	4
II. States on the Triangle and the Circle: Two Dimensional Case	8
A. Solutions on the Edge	10
B. Mappings and Ladder Operators	11
C. The Equilateral Triangle States: Comparison of Edge States vs the Inner States	13
III. Triangle and Circle: Topology and States	15
IV. Coherent States of the Triangle	17
A. Test for the Cyclic Group C_3	18
V. The Metaplectic Group $Mp(n)$ Action: Classicalization	19
A. The Minimal Group Representation and Coherent States in the Triangle	20
VI. Topological Separation Conditions of the Even and Odd Sectors $s = 1/4$ and $s = 3/4$	23
VII. Generalization of the Bargmann Representation and the Metaplectic Symmetry	24
VIII. Remarks and Conclusions	25
IX. Acknowledgements	28
X. Appendix: coset coherent states alternative normalization	29
XI. AUTHOR DECLARATIONS	29
A. Conflict of Interest	29
B. Author Contributions	29
XII. DATA AVAILABILITY	30
References	30

I. INTRODUCTION AND RESULTS

Quantum theory is at the center of science and technology today: The great success of Quantum theory and its deep and wide impact transcends physics and its applications: See for example Refs [1], [2], [3], [4] [5], [6]. While the quantum wave nature of particles and the intrinsic quantum uncertainty principle were mainly about the first quantum revolution, the superposition principle and quantum entanglement are at the heart of the second quantum revolution at work.

As we have already pointed out Ref [7], while quantum research is rapidly evolving in many different directions and disciplines, it is more and more necessary to have a precise modern physical understanding and clear computational framework for **the classical dual content of quantum theory**: This is important for both: from the conceptual and quantum interpretation measurements until quantum technologies and computation research. Therefore, one fundamental question in Quantum theory with interest for its conceptual, observational and experimental research is the following:

Under which conditions Quantum theory does **appear Classical, namely which are the Classical dual sectors of the Quantum world.**

Classical states are a particular case of Quantum theory and are dual states in the precise sense of the general classical- quantum duality of Nature. Recently, in ApL Quantum 2025 Ref [8], we provided a precise answer to this problem within a novel approach: The minimal group representation principle, which is uniquely realized by the Metaplectic group $Mp(2d)$. This group is the double covering of the Symplectic group $Sp(2d)$ and its action immediately *classicalizes* the system. We performed an extensive study with different types of quantum states on the circle and on the cylinder from which emerged too that $Mp(2d)$ is the *symmetry group of the general classical-quantum duality of Nature*. In the same lines, in [9] we went beyond in our study of the Classical sectors of Quantum theory by investigating the **Entanglement** for the quantum-classical dual states with topologies on the circle and on the cylinder and different types of coherent (coset and non coset) states, finding as results the **Entanglement and Classicalization, and the relationship between them**.

Consequently we found the bridge between the classical and quantum information processings and relates to a real-world problem.

In this work, within the main guidelines of our framework [7], we will examine the effect of the geometry on the various observables in the quantum field and its classification. To this end, the case of the triangle (as the simplest polygon) is considered here. The action of the $Mp(n)$ group which is the group with the Minimal Group Representation (MGR) will play a fundamental role in the analysis, as we have done successfully in the case of the circle previously considered in Ref[8].

The main concepts in our analysis are based on the following :

Discretization arises naturally and directly from the basic states of the metaplectic representations: the decomposition of the $Mp(2)$ group into its two irreducible representations span both: the *even* $|2n\rangle$ and *odd* $|2n + 1\rangle$ states respectively, ($n = 1, 2, 3 \dots$) of the harmonic oscillator, totally covered by the metaplectic group. The two $Mp(2)$ irreducible subspaces contain *both*: the quantum and the classical dual sectors. For $n \rightarrow \infty$, the spectrum becomes naturally continuum as it must be.

A quantum state **completely classicalizes** its inherent quantum structure **only** under the action of the **$Mp(n)$ (metaplectic) Group**, (Minimal Representation Group). **Classicalization** is explicit in the decreasing exponential factors for large n arising in the $Mp(2)$ projections of the states: screenings e^{-2n} , $e^{-(2n+1/2)}$ or e^{-2n^2} , $e^{-(2n+1/2)^2}$ (depending on the topology, circle or cylinder states respectively).

The **Classical-Quantum Duality** is realized in the $Mp(n)$ symmetry because of the complete covering of the Hilbert space: Each of the two, *even* $\mathcal{H}_{(+)}$ and *odd* $\mathcal{H}_{(-)}$ sectors are local coverings, their sum being global, completely covering the *whole* Hilbert space $\mathcal{H} = \mathcal{H}_{(+)} \oplus \mathcal{H}_{(-)}$.

The two (+) and (-) sectors are classical-quantum duals of each other and are **entangled**. This is also important in order to include gravity at the Planck scale and beyond: quantum space-time and classical-quantum gravity duality, Refs [10], [11], [12], [13], [14] which is general, irrespective of the number or type of space-time dimensions or manifolds (with or without compactifications).

In this paper our focus and results are the following:

(1) **By analogy** and for comparison with the case of the circle, we solved here the two-dimensional Schrodinger equation for the equilateral triangular network with the solution

:

$$\begin{aligned} \Phi_{2d}(x, y)|_{edge} = & \cos \left[(2p + q) \frac{2\pi y}{\sqrt{3}a} \right] \sin \left[q \frac{2\pi x}{a} \right] - \\ & - \sin \left[p \frac{2\pi x}{a} \right] \cos \left[(2q + p) \frac{2\pi y}{\sqrt{3}a} \right] - \\ & - \sin \left[(p + q) \frac{2\pi x}{a} \right] \cos \left[(p - q) \frac{2\pi y}{\sqrt{3}a} \right], \end{aligned}$$

where the parameter a is the side of the triangle, q and p are characteristics numbers which parametrize it, and the energies are:

$$E_{pq}|_{edge} = (p^2 + pq + q^2) E_{1,0}$$

Notice that this is the dual to the triangular recent solution of [15]

(2) The new general ladder operators of the item **(1)** were explicitly constructed for the first time, for the case $q = 0$ and for one of the sides

$$\Phi_{p-n,0}(w) = \underbrace{\left[\cos(nw) - \frac{\sin(nw)}{p} \partial_w \right]}_{A_{-n}} \Phi_{p,0}(w) \quad (1)$$

that allows to construct the eigenstates of the operator A_{-1} (see (1)) with eigenvalue a , with the result:

$$f(pw) = a \sin(pw) \left(\frac{\sin w}{(\tan w/2)^a} \right)^p \quad (2)$$

where w is one of the three convenient coordinates (u, v, w) that symmetrize the expressions defining the equilateral triangle boundary conditionsthe expressions Similar expressions such as Eq.(2) hold for u and v .

(3) The coset coherent states for the triangle are explicitly constructed here with the action of the dihedral group D_3 (six generators) on the circle coset coherent states constructed in Ref [8] as fiducial, obtaining

$$|\alpha_{D_3}, \varphi\rangle = \mathcal{N} \sum_{r=1}^6 |\alpha_r, \varphi\rangle$$

with α_r defining the complex index of the coherent states under the action of $D_3 : (g_{D_3})_r \alpha \equiv \alpha_r$ \mathcal{N} is a nomalization factor. This normalization is important (despite its complexity) and,

in the case of coset coherent states, depends on the chosen fiducial vector. Our fiducial vector ensures normalizability in sharp contrast to having the London state as fiducial.(see [8]).

(4) The probability (square of the wave function) for the coherent state found also demonstrates overlap (quantum interaction) between the different sides of the triangle.

(5) Applying the action of the metaplectic group (Minimal Group Representation) splits the Hilbert space into *even* and *odd* sectors, revealing the very deep quantum space-time structure. There, one can see how, the resulting probability has a clear entanglement structure between projected sectors (even and odd) and the respective sides. The obtained probabilities are given by:

$$\begin{aligned}
|\langle \alpha_{C_3}, \varphi | \Psi(\omega) \rangle|^2 &= \mathcal{N}^2 (1 - |\omega|^2)^{1/2} \tag{3} \\
&\left\{ \sum_{r=s=1}^3 \left[\cosh(|z'_r/2|^2) + (1 - |\omega|^2) \sinh(|z'_r/2|^2) + (1 - |\omega|^2)^{1/2} \sum_{n=0,1,2..} \frac{(|z'_r|^2/4)^{2n} \operatorname{Re} z'_r}{\sqrt{(2n)!(2n+1)!}} \right] + \right. \\
&\quad \left. + \sum_{r \neq s=1}^3 2 \left[\cosh\left(\frac{z'_r z'_s{}^* + z'_s z'_r{}^*}{4}\right) + (1 - |\omega|^2) \sinh\left(\frac{z'_r z'_s{}^* + z'_s z'_r{}^*}{4}\right) \right] \cosh\left(\frac{z'_r z'_s{}^* - z'_s z'_r{}^*}{4}\right) + \right. \\
&\quad \left. + (1 - |\omega|^2)^{1/2} \sum_{n=0,1,2..} \frac{(z'_r z'_s{}^*/4)^{2n} (z'_r + z'_s)}{\sqrt{(2n)!(2n+1)!}} \right\}
\end{aligned}$$

Here $z'_r = \omega e^{i(\varphi - \alpha_r^*/2)}$ (analogously for z'_s) where ω is an analytic function on the disk (according to the Bargmann representation).

(6) The maximum separation (purity) conditions in the probability expression -after the metaplectic group action has been applied- imply particular relationships between the metaplectic projection parameters. The expression of the probability appears as the sum of even and odd probabilities (without mixed terms) if it is satisfied that: $z'_r = -z'_s{}^*$ for $r \neq s$ and $\operatorname{Re} z'_r = 0$ for $r = s$.

(i) Case $\operatorname{Re} z'_r = 0$: By dropping the subindex r in the final expression and decomposing α_r and ω in their real and imaginary parts, we get :

$$\begin{aligned}
z'_r &= \omega e^{i(\varphi - \alpha_r^*/2)} \\
&= e^{-\alpha_{rI}/2} \{ [\omega_R \cos(\varphi - \alpha_{rR}/2) - \omega_I \sin(\varphi - \alpha_{rR}/2)] + \\
&\quad + i [\omega_I \cos(\varphi - \alpha_{rR}/2) + \omega_R \sin(\varphi - \alpha_{rR}/2)] \}
\end{aligned}$$

Consequently

$$\operatorname{Re} z'_r = 0 \implies \omega_R = \omega_I \tan(\varphi - \alpha_{rR}/2)$$

$$z'_r = 2 e^{-\alpha_{rI}/2} i \omega_I \sin(\varphi - \alpha_{rR}/2)$$

This case is analog to the purity condition in the circle.

(ii) The case $z'_r = -z'^*_s$

This case corresponds to anti-duality condition in the complex sense. Knowing that

$$z'^*_s = \sigma^* e^{-i(\varphi' - \alpha_s/2)}$$

Consequently:

$$\omega e^{i(\varphi - \alpha_r^*/2)} = -\sigma^* e^{-i(\varphi' - \alpha_s/2)}$$

$$\frac{\omega \sigma}{|\sigma|^2} = -e^{-i[(\varphi' + \varphi) - (\alpha_s + \alpha_r^*)/2]}$$

Where the functions on the disk namely ω and σ are linked exponentially with the $\varphi', \varphi, \alpha_s, \alpha_r^*$ operating as control parameters.

In Section II, the 2-d Schrödinger equation is solved for a triangular lattice. The main difference with works [15],[16] is that they solve not for the triangular edge, but for the interior of the enclosure. This is fundamental to establishing a connection with the topological problem that we treat in Section III, where the circle will be the foundation. In section IV, coherent states will be constructed for the equilateral triangle by mean of the action of the dihedral group D3 on the coset E(2)/T2 (with our coset coherent states for the circle as fiducial). Section V is dedicated to introducing the Minimal Group Representation principle (MGRP), showing the action of the metaplectic group on the coherent states of Section IV and the classicalization of the quantum system. The topological separation conditions (maximum purity) under the action of Mp(2) are given in Section VI and in Section VII a generalization in the context of the MGRP of the Bargmann representation, not previously introduced in the literature, is presented. Finally in Section VIII we provide our Remarks and Conclusions

II. STATES ON THE TRIANGLE AND THE CIRCLE: TWO DIMENSIONAL CASE

The equilateral triangle case was treated repeatedly in the literature [15] starting from the 2d-Schrodinger equation (stationary case) in the usual way:

$$-\frac{\hbar^2}{2m} (\partial_x^2 + \partial_y^2) \Phi_{2d} = E\Phi_{2d}$$

$$\mathcal{H}\Phi_{2d} = E\Phi_{2d}$$

where the states within the triangle respond to Dirichlet conditions for the boundaries (as in the case of a waveguide).

The case is non-separable but allows exact solutions, and the edges of the triangle are taken as regions where the solution must be zero. As a first step, due that we will relate to the circle, the conditions here **will be precisely the opposite**: the function exists at the boundaries of the triangular region going to zero otherwise because the case so far is two-dimensional:

$$\Phi_{2d}(x, y) \neq 0 \rightarrow \begin{cases} y = 0 \\ y = \sqrt{3}x \\ y = \sqrt{3}(a - x) \end{cases} \quad (4)$$

$$\Phi_{2d}(x, y) = 0, \quad \text{otherwise}$$

Here, a is the side of the triangle. These conditions can be written in a symmetrical way for equilateral triangle with the following redefinitions [15]

$$u = \left(\frac{2\pi}{A}\right) y \quad (5)$$

$$v = \left(\frac{2\pi}{A}\right) \left(-\frac{y}{2} + \frac{\sqrt{3}}{2}x\right)$$

$$w = \left(\frac{2\pi}{A}\right) \left(-\frac{y}{2} - \frac{\sqrt{3}}{2}x\right) + 2\pi$$

with the height of the equilateral triangle: $A = \frac{\sqrt{3}}{2}a$. Consequently, the conditions Eqs(4) take the form

$$\Phi_{2d}(x, y) \neq 0 \rightarrow \begin{cases} v = 2\pi - w, & u = 0 \\ w = 2\pi - u, & v = 0 \\ u = 2\pi - v, & w = 0 \end{cases} \quad (6)$$

$$\Phi_{2d}(x, y) = 0, \quad \text{otherwise}$$

A. Solutions on the Edge

The edge solutions in that case for the irreducible representation of the equilateral triangle symmetry A_1 (still two-dimensional) will take the form

$$\begin{aligned}\Phi_{2d}(x, y)|_{edge} &= \cos \left[(2p + q) \frac{2\pi y}{\sqrt{3}a} \right] \sin \left[q \frac{2\pi x}{a} \right] - \\ &\quad - \sin \left[p \frac{2\pi x}{a} \right] \cos \left[(2q + p) \frac{2\pi y}{\sqrt{3}a} \right] - \\ &\quad - \sin \left[(p + q) \frac{2\pi x}{a} \right] \cos \left[(p - q) \frac{2\pi y}{\sqrt{3}a} \right],\end{aligned}$$

$$\mathcal{H} \Phi_{2d}(x, y)|_{edge} = E_{pq} \Phi_{2d}(x, y)|_{edge}$$

with the Hamiltonian eigenvalues (energies) as

$$E_{pq} = (p^2 + pq + q^2) E_{10}$$

where

$$E_{10} = \left(\frac{\hbar\pi}{a} \right)^2 \frac{8}{3m} = \left(\frac{\hbar\pi}{A} \right)^2 \frac{2}{m}$$

and notice that

$$E_{0q} = 0$$

Let us notice too that the solution as a function of p and q is not symmetrical because:

$$\Phi_{2d}(x, y)|_{edge} \equiv \Phi_{p,q}|_{edge} \rightarrow \Phi_{0,q}|_{edge} = 0$$

and

$$\Phi_{p,0}|_{edge} = -2 \sin \left[p \frac{2\pi x}{a} \right] \cos \left[p \frac{2\pi y}{\sqrt{3}a} \right] \quad (7)$$

(i) As a function of the convenient variables (v,w) it takes the compact form

$$\Phi_{p,0}|_{edge} = \sin(pw) - \sin(pv) \quad (8)$$

which is simplified to a dependency on w using the conditions Eqs (6)

$$\Phi_{p,0}|_{edge} = 2 \sin(pw) \quad (9)$$

This last expression will be important in the construction of the coherent states in this too simplified case.

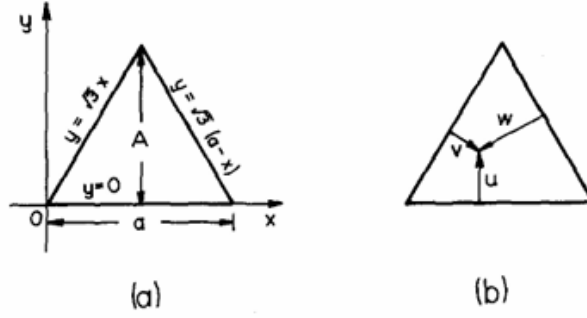


FIG. 1: u, v, w are coordinates that symmetrize the expressions of the boundary conditions of the equilateral triangle and define a point of it. Note that the edges are defined by expressions (5) with $u=0, v=0$ and $w=0$ respectively.

(ii) As a function of the variables (u, w) we must to consider

$$\begin{aligned} \frac{A}{2\pi} u &= y \\ -\frac{A}{\pi\sqrt{3}} [(w - 2\pi) + u/2] &= x \end{aligned}$$

$$\Phi_{p,0}|_{edge} = 2 \sin [p[(w - 2\pi) + u/2]] \cos [pu/2] \quad (10)$$

$$= \{ \sin [p[(w - 2\pi) + u]] + \sin [p(w - 2\pi)] \} \quad (11)$$

(iii) As a function of the variables (u, v) we must consider

$$\begin{aligned} \frac{A}{2\pi} u &= y \\ \frac{A}{\pi\sqrt{3}} (v + u/2) &= x \end{aligned}$$

$$\Phi_{p,0}|_{edge} = -2 \sin [p(w + u/2)] \cos [pu/2] \quad (12)$$

$$= -\{ \sin [p(w + u)] + \sin [pw] \} \quad (13)$$

Let us now consider the mappings of the triangle edge states and the ladder operators

B. Mappings and Ladder Operators

The triangle problem, even in its simplest form (billiards or waveguides), is a non-separable but integrable problem. It is possible, however, to construct differential operators

that map states $\Phi_{p,0}|_{edge}$ of different values of p . For example

$$\begin{aligned} \Phi_{p,0}(w) &\rightarrow \Phi_{p+n,0}(w) \\ \Phi_{p+n,0}(w) &= \underbrace{\left[\cos(nw) + \frac{\sin(nw)}{p} \partial_w \right]}_{A_n} \Phi_{p,0}(w) \end{aligned} \quad (14)$$

In order to increase p by one unit, starting from a known fiducial state we have:

$$\Phi_{p+1,0}(w) = A_1 \Phi_{p,0}(w)$$

Similarly, we have a reverse mapping

$$\Phi_{p,0}(w) \rightarrow \Phi_{p-n,0}(w)$$

which is formally of the form

$$\Phi_{p-n,0}(w) = \underbrace{\left[\cos(nw) - \frac{\sin(nw)}{p} \partial_w \right]}_{A_{-n}} \Phi_{p,0}(w) \quad (15)$$

To lower p by one unit, starting from a known fiducial state we have:

$$\Phi_{p-1,0}(w) = A_{-1} \Phi_{p,0}(w)$$

The question now is how to define, starting from a known ground state, a generic state "n". The standard case, for example, is well known: $|n\rangle = \sum \frac{(a^+)^n}{\sqrt{n!}} |0\rangle$, now considering the form Eq.(14) and making steps one by one taking a fiducial state $\Phi_{p,0}(w) = \sin(pw)$ with $p \geq 1 \in \mathbb{N}$:

$$\Phi_m(w) \equiv \Phi_{p+m,0}(w) = \prod_{n=1}^m \left[\cos w + \frac{\sin w}{p+n-1} \partial_w \right] \Phi_{p,0}(w)$$

e.g. $\Phi_{p+3,0}(w) = \sin[(p+3)w]$ we have:

$$\begin{aligned} \Phi_{p+3,0}(w) &= \prod_{n=1}^3 \left[\cos w + \frac{\sin w}{p+n-1} \partial_w \right] \Phi_{p,0}(w) \\ \Phi_{p+3,0}(w) &= \underbrace{\left(\cos w + \frac{\sin w}{p+2} \partial_w \right) \left(\cos w + \frac{\sin w}{p+1} \partial_w \right) \left(\cos w + \frac{\sin w}{p} \partial_w \right)}_{\Phi_{p,0}(w) \rightarrow \Phi_{p+1,0}(w)} \Phi_{p,0}(w) \\ &\quad \underbrace{\hspace{10em}}_{\Phi_{p+1,0}(w) \rightarrow \Phi_{p+2,0}(w)} \\ &\quad \underbrace{\hspace{15em}}_{\Phi_{p+2,0}(w) \rightarrow \Phi_{p+3,0}(w)} \end{aligned}$$

$$\Phi_{p+3,0}(w) = \sin[(p+3)w]$$

By acting with the operator $-\partial_w^2$ on Eq.(14)

$$\begin{aligned} -\partial_w^2 \Phi_{p+n,0}(w) &= (p+n)^2 \Phi_{p+n,0}(w) \\ &= (p+n)^2 A_n \Phi_{p,0}(w) \end{aligned}$$

The commutation relations are easily derived, taking the operator $-\partial_w^2$ as our N operator :

$$[N, A_1] = (2p+1) A_1$$

$$[N, A_{-1}] = -(2p-1) A_{-1}$$

Notice that the commutation relations are non canonical (e.g. the Jacobi identities are not fulfilled). The fiducial state that is annihilated by A_{-1} is the state $\Phi_{1,0}(w)$

Eigenstates of the operator A_{-1} with eigenvalue a take the form

$$f(pw) = a \sin(pw) \left(\frac{\sin w}{(\tan w/2)^a} \right)^p$$

similarly for coordinates u and v . The norm of this eigenstate is represented in the figure (2).

C. The Equilateral Triangle States: Comparison of Edge States vs the Inner States

We will analyze here **only** the solutions with symmetry under the irreducible representation A_1

Our states are geometrically defined with their maxima at the edges of the triangle and going to zero inside the triangle.

In the Figure (3) We have the probability for $\Phi_{2,1}|_{edge}$: we can clearly see the peaks of the function at the triangular edges and going to zero in the central regions. The density plot of this probability $|\Phi_{2,1}|_{edge}|^2$ is given in the Figure (4). We compare with the reference case [15] with waveguide-type boundary conditions (where the function vanishes at the boundary) e.g.

$$\Phi_{2d}(x, y) = 0 \rightarrow \begin{cases} y = 0 \\ y = \sqrt{3}x \\ y = \sqrt{3}(a-x) \end{cases}$$

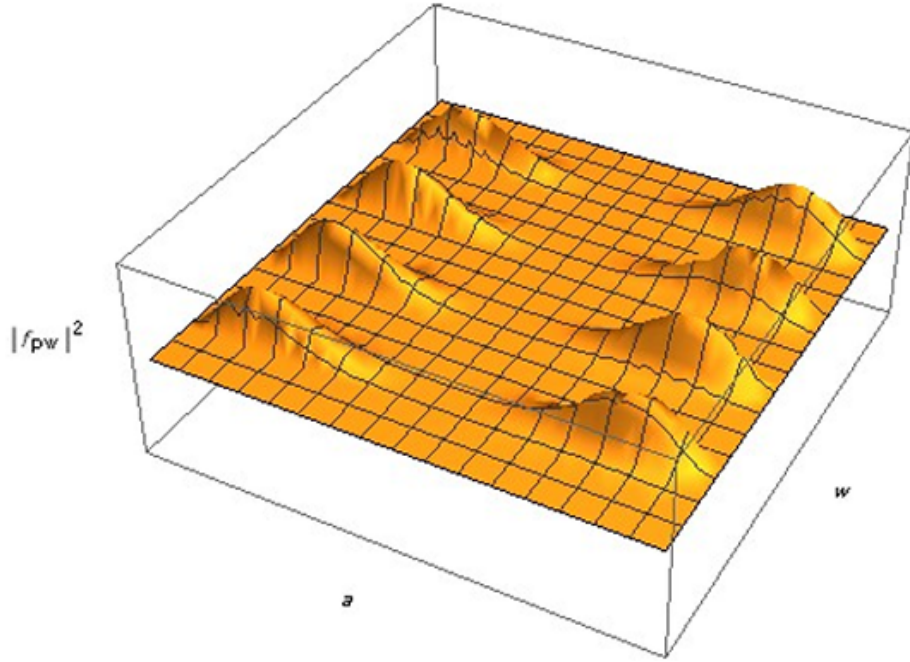


FIG. 2: Norm of the eigenstates $f(pw)$ of the operator A_{-1} with eigenvalue a .

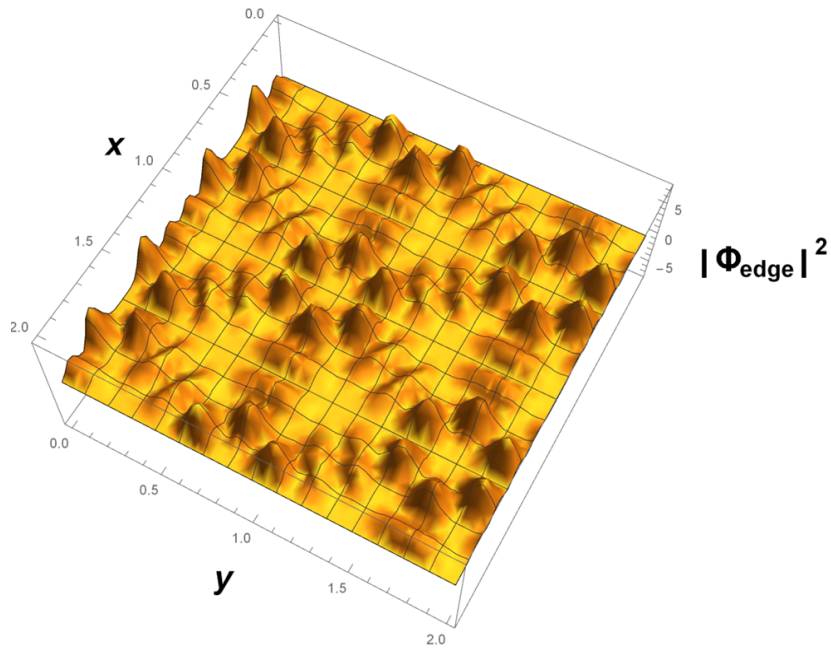


FIG. 3: In this Figure we have the probability for $\Phi_{2,1}|_{edge}$: we can clearly see the peaks of the function at the triangular edges and going to zero in the central regions.

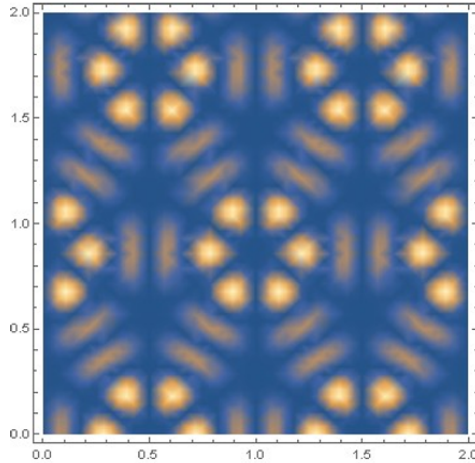


FIG. 4: Here we have the density plot of the probability for $\Phi_{2,1}|_{edge}$ described in Fig. 1.

These states are geometrically defined with their maxima at the center of the triangle and going to zero in the edges. In the Figure (5) we have the probability for $\Phi_{2,1}$: we can clearly see the peaks of the function at the center of the triangle and going to zero in the edges in all the 2-dimensional patterns. The density plot of this probability $|\Phi_{2,1}|^2$ is given in the Figure (6).

III. TRIANGLE AND CIRCLE: TOPOLOGY AND STATES

For the Triangle states and the relation with the circle states (edges), the main points are

(1) We will concentrate in the edge: the system turns to be 1-dimensional acquiring a topological character.

(2) For symmetry we take an equilateral triangle.

(3) The side of the triangle, namely a , is constrained to the perimeter of the unitary circle by the relation $3a = 2\pi \rightarrow a = \frac{2\pi}{3}$

(4) The coordinates of the plane in the bidimensional (surface) case now will be those of the unitary circle

$$x = \cos \varphi \qquad y = \sin \varphi$$

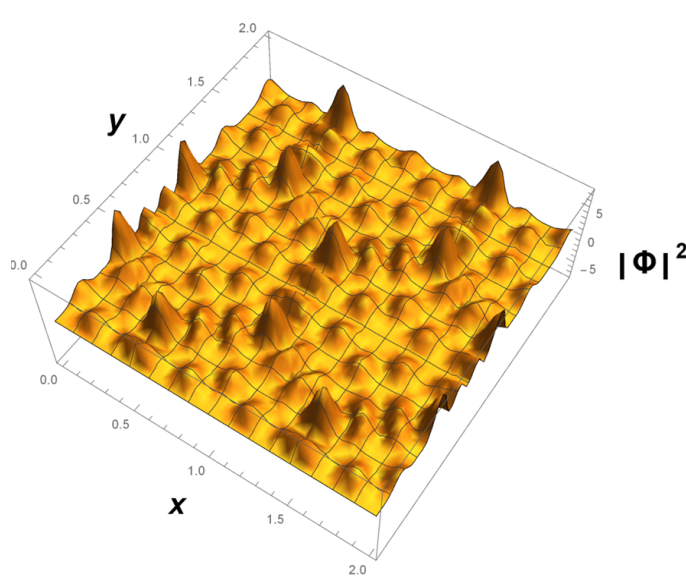


FIG. 5: In this Figure we have the probability for $\Phi_{2,1}$: we can clearly see the peaks of the function at the triangular center and going to zero in the edge regions in all the 2d pattern.

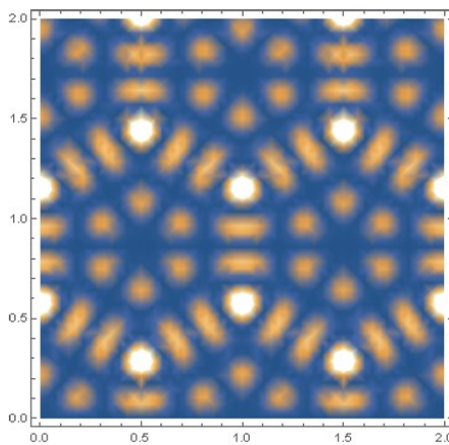


FIG. 6: Here we have the density plot of the probability for $\Phi_{2,1}$ described in Fig. 3.

Therefore, the solution is now

$$\begin{aligned} \Phi_{1d} = & \cos \left[\sqrt{3} (2p + q) \sin \varphi \right] \sin [3q \cos \varphi] - \\ & - \sin [3(p + q) \cos \varphi] \cos \left[\sqrt{3} (2q + p) \sin \varphi \right] - \\ & - \sin [3(p + q) \cos \varphi] \cos \left[\sqrt{3} (p - q) \sin \varphi \right] \end{aligned}$$

IV. COHERENT STATES OF THE TRIANGLE

Our starting point is the coset coherent states for the circle, which will be used as a fiducial state, using the specific coset $E(2)/T(2)$ being $T(2)$ the 2 dimensional translation group:

$$|\alpha, \varphi\rangle \frac{1}{2\pi} S(\alpha, \varphi) \underbrace{\sum_{n=0,1,2,\dots} e^{-i(\varphi-\alpha/2)} |n\rangle}_{|\varphi-\alpha/2\rangle}$$

$$S(\alpha, \varphi) = A_+ \cos \alpha + A_- \sin \alpha$$

$$A_{\pm} = (\cos \varphi \pm \sin \varphi) x + (\mp \cos \varphi + \sin \varphi) y$$

In the second step, we applied the action of the dihedral group D_3 to $\alpha \in \mathbb{C}$ (which characterizes the coherent state $E(2)/T(2)$) defining the corresponding orbits for the triangle.

The D_3 group, which is the dihedral group, has 6 elements, of which 3 of them are from the cyclic group C_3 and 3 belong to the reflections in the equilateral triangle:

$$\begin{aligned} g_1 &= \begin{pmatrix} 1 & 0 \\ 0 & 1 \end{pmatrix}, \quad g_4 = \begin{pmatrix} -1 & 0 \\ 0 & 1 \end{pmatrix} \\ g_2 &= \begin{pmatrix} -1 & -\sqrt{3} \\ \sqrt{3} & -1 \end{pmatrix}, \quad g_5 = \begin{pmatrix} 1 & -\sqrt{3} \\ -\sqrt{3} & -1 \end{pmatrix} \\ g_3 &= \begin{pmatrix} -1 & \sqrt{3} \\ -\sqrt{3} & -1 \end{pmatrix}, \quad g_6 = \begin{pmatrix} 1 & \sqrt{3} \\ \sqrt{3} & -1 \end{pmatrix} \end{aligned}$$

these elements of D_3 operate on $\alpha = \alpha_R + i\alpha_I$ of the complex field represented as a doublet [16]:

$$\alpha = \begin{pmatrix} \alpha_R \\ \alpha_I \end{pmatrix}$$

namely

$$\begin{aligned} \alpha_1 &= \alpha \\ \alpha_2 &= e^{\frac{2\pi i}{3}} \alpha \\ \alpha_3 &= e^{-\frac{2\pi i}{3}} \alpha \\ \alpha_4 &= -\alpha^* \\ \alpha_5 &= \frac{1}{2} (\alpha_R - \sqrt{3}\alpha_I) - \frac{i}{2} (\alpha_I + \sqrt{3}\alpha_R) \\ \alpha_6 &= \frac{1}{2} (\alpha_R + \sqrt{3}\alpha_I) + \frac{i}{2} (-\alpha_I + \sqrt{3}\alpha_R) \end{aligned} \tag{16}$$

The coherent state in this case, respecting the symmetry of the equilateral triangle, can be written by the sequence

$$|\alpha_{D_3}, \varphi\rangle = \mathcal{N} \sum_{r=1}^6 |\alpha_r, \varphi\rangle$$

where \mathcal{N} is a normalization constant to be determined and $|\alpha_r, \varphi\rangle$ the normalized coherent states:

$$|\alpha_r, \varphi\rangle = \sqrt{1 - e^{-\text{Im} \alpha_r}} e^{i \arg S(\alpha_r, \varphi)} \sum_{n=0,1,2,\dots} e^{-i(\varphi - \alpha_r/2)n} |n\rangle$$

here the overlap is

$$\begin{aligned} \langle \alpha_s, \varphi | \alpha_r, \varphi \rangle &= \mathcal{A}(\alpha_r) \mathcal{A}(\alpha_s) e^{-i \arg S(\alpha_s, \varphi)} e^{i \arg S(\alpha_r, \varphi)} \sum_{n,m=0,1,2,\dots} e^{i(\varphi - \alpha_s^*/2)m} e^{-i(\varphi - \alpha_r/2)n} \langle m | |n\rangle \\ &= \mathcal{A}(\alpha_r) \mathcal{A}(\alpha_s) e^{-i \arg S(\alpha_s, \varphi)} e^{i \arg S(\alpha_r, \varphi)} \sum_{n=0,1,2,\dots} e^{in(\alpha_r - \alpha_s^*)/2} \\ &= \mathcal{A}(\alpha_r) \mathcal{A}(\alpha_s) \frac{e^{-i(\arg S(\alpha_s^*, \varphi) - \arg S(\alpha_r, \varphi))}}{1 - e^{i(\alpha_r - \alpha_s^*)/2}} \\ &= \mathcal{A}(\alpha_r) \mathcal{A}(\alpha_s) \frac{e^{-i \arg S(\alpha_s^*, \varphi) - \arg S(\alpha_r, \varphi)}}{1 - e^{i \text{Re}(\alpha_r - \alpha_s)/2 - \text{Im}(\alpha_r + \alpha_s)/2}} \end{aligned}$$

where we have defined :

$$\mathcal{A}(\alpha_r) \equiv \sqrt{1 - e^{-\text{Im} \alpha_r}}, \quad \mathcal{A}(\alpha_s) \equiv \sqrt{1 - e^{-\text{Im} \alpha_s}} \quad (17)$$

A. Test for the Ciclic Group C_3

In order to simplify our task, we will take the cyclic subgroup C_3 of the dihedral group. Consequently, we take $r=1,2,3$, $|\alpha_r, \varphi\rangle \rightarrow$ normalized. Then the coherent state is defined **exactly** as

$$\begin{aligned} |\alpha_{C_3}, \varphi\rangle &= \mathcal{N} \left(\sum_{r=1}^3 |\alpha_r, \varphi\rangle \right) \\ &= \mathcal{N} (|\alpha_1, \varphi\rangle + |\alpha_2, \varphi\rangle + |\alpha_3, \varphi\rangle) \end{aligned} \quad (18)$$

$$\langle \alpha_{C_3}, \varphi | \alpha_{C_3}, \varphi \rangle = \mathcal{N}^2 [3 + 2 (\text{Re} \langle \alpha_1, \varphi | \alpha_2, \varphi \rangle + \langle \alpha_3, \varphi | \alpha_2, \varphi \rangle + \langle \alpha_1, \varphi | \alpha_3, \varphi \rangle)]$$

Consequently, the normalization function can be determined

$$\mathcal{N}^2 = \frac{1}{3 \left[1 + \frac{2}{3} (\text{Re} \langle \alpha_1, \varphi | \alpha_2, \varphi \rangle + \text{Re} \langle \alpha_3, \varphi | \alpha_2, \varphi \rangle + \text{Re} \langle \alpha_1, \varphi | \alpha_3, \varphi \rangle) \right]}$$

where

$$\text{Re} \langle \alpha_1, \varphi | | \alpha_2, \varphi \rangle = \frac{\cos [\arg S (\alpha_1^*, \varphi) - \arg S (\alpha_2, \varphi)] \sqrt{(1 - e^{\alpha_{1I}}) (1 - e^{-\alpha_{2I}})}}{1 - \cos \left(\frac{\alpha_{2R} - \alpha_{1R}}{2} \right) \exp \left(\frac{\alpha_{2I} + \alpha_{1I}}{2} \right)} =$$

$$\text{Re} \langle \alpha_3, \varphi | | \alpha_1, \varphi \rangle = \frac{\cos [\arg S (\alpha_3^*, \varphi) - \arg S (\alpha_1, \varphi)] \sqrt{(1 - e^{\alpha_{3I}}) (1 - e^{-\alpha_{1I}})}}{1 - \cos \left(\frac{\alpha_{1R} - \alpha_{3R}}{2} \right) \exp \left(\frac{\alpha_{1I} + \alpha_{3I}}{2} \right)} =$$

$$\text{Re} \langle \alpha_2, \varphi | | \alpha_3, \varphi \rangle = \frac{\cos [\arg S (\alpha_2^*, \varphi) - \arg S (\alpha_3, \varphi)] \sqrt{(1 - e^{\alpha_{2I}}) (1 - e^{-\alpha_{3I}})}}{1 - \cos \left(\frac{\alpha_{2R} - \alpha_{3R}}{2} \right) \exp \left(\frac{\alpha_{2I} + \alpha_{3I}}{2} \right)}$$

$$\alpha_1 = \alpha_R + i\alpha_I \equiv \alpha_{1R+} i\alpha_{1I} \quad (19)$$

$$\alpha_2 = -\frac{1}{2} \left(\alpha_R + \sqrt{3}\alpha_I \right) + \frac{i}{2} \left(\sqrt{3}\alpha_R - \alpha_I \right) \equiv \alpha_{2R+} i\alpha_{2I} \quad (20)$$

$$\alpha_3 = -\frac{1}{2} \left(\alpha_R - \sqrt{3}\alpha_I \right) - \frac{i}{2} \left(\sqrt{3}\alpha_R + \alpha_I \right) \equiv \alpha_{3R+} i\alpha_{3I} \quad (21)$$

and

$$S (\alpha_1, \varphi) = S (\alpha, \varphi) = x [\cos (\alpha + \varphi) + \sin (\alpha + \varphi)]$$

$$S (\alpha_2, \varphi) = S \left(e^{\frac{2\pi i}{3}} \alpha, \varphi \right) = x [-(-1 + \sqrt{3}) \cos ((-1)^{2/3} \alpha + \varphi) + (1 + \sqrt{3}) \sin ((-1)^{2/3} \alpha + \varphi)]$$

$$\begin{aligned} S (\alpha_3, \varphi) = S \left(e^{-\frac{2\pi i}{3}} \alpha, \varphi \right) = & \left(-\frac{2\pi\sqrt{3}}{3} + (1 + \sqrt{3})x \right) \cos ((-1)^{1/3} \alpha - \varphi) + \\ & + \left(-\frac{2\pi\sqrt{3}}{3} + (-1 + \sqrt{3})x \right) \sin ((-1)^{1/3} \alpha - \varphi) \end{aligned}$$

V. THE METAPLECTIC GROUP $\text{Mp}(N)$ ACTION: CLASSICALIZATION

Again, let us look at the sector $s = 1/4$ of the Hilbert space spanned by the $\text{Mp}(2)$ coherent states (unnormalized), the basic state is

$$|\Psi^{(+)}(\omega)\rangle = (1 - |\omega|^2)^{1/4} \sum_{n=0,1,2..} \frac{(\omega/2)^{2n}}{\sqrt{2n!}} |2n\rangle$$

On the other hand:

$$\langle \alpha, \varphi | = \mathcal{N}^* \sum_{n=0,1,2..} e^{i(\varphi - \alpha^*/2)n} \langle n | \quad (22)$$

Therefore, with all the definitions above, and in principle excluding the normalization \mathcal{N} we have

$$\langle \alpha, \varphi | \Psi^{(+)}(\omega)\rangle = \frac{(1 - |\omega|^2)^{1/4}}{\sqrt{2\pi}} \sum_{m=0,1,2..} \sum_{n=0,1,2..} \frac{(\omega/2)^{2n}}{\sqrt{2n!}} e^{i(\varphi - \alpha^*/2)m} \langle m | |2n\rangle \quad (23)$$

$$\begin{aligned} \langle \alpha, \varphi | \Psi^{(+)}(\omega)\rangle &= \frac{(1 - |\omega|^2)^{1/4}}{\sqrt{2\pi}} \sum_{n=0,1,2..} \frac{(\omega e^{i(\varphi - \alpha^*/2)}/2)^{2n}}{\sqrt{2n!}} = \\ &= \frac{(1 - |\omega|^2)^{1/4}}{\sqrt{2\pi}} \sum_{n=0,1,2..} \frac{(z'/2)^{2n}}{\sqrt{2n!}} \end{aligned} \quad (24)$$

with

$$\omega e^{i(\varphi - \alpha^*/2)} = z e^{-i\alpha^*/2} \equiv z'$$

: the analytic function in the disc now is now modified by the complex phase $\varphi - \alpha^*/2$.

In a similar same way for the sector $s = 3/4$ we have:

$$\begin{aligned} \langle \alpha, \varphi | \Psi^{(-)}(\omega)\rangle &= \frac{(1 - |\omega|^2)^{3/4}}{\sqrt{2\pi}} \sum_{n=0,1,2..} \frac{(\omega e^{i(\varphi - \alpha^*/2)}/2)^{2n+1}}{\sqrt{(2n+1)!}} = \\ &= \frac{(1 - |\omega|^2)^{3/4}}{\sqrt{2\pi}} \sum_{n=0,1,2..} \frac{(z'/2)^{2n+1}}{\sqrt{(2n+1)!}} \end{aligned} \quad (25)$$

A. The Minimal Group Representation and Coherent States in the Triangle

Notice that by taking the scalar product between the found coset coherent state for the triangle and the states of $Mp(2)$, we obtain two non-equivalent expansions in terms of analytical functions on the disk for the sectors of the minimal representation $s = 1/4, 3/4$, even and odd sectors respectively, in the eigenstates n of the harmonic oscillator. Consequently, by defining

$$\omega e^{i(\varphi - \alpha_r^*/2)} \equiv z'_r$$

We have

$$\langle \alpha_r, \varphi | \Psi(\omega) \rangle \begin{cases} (1 - |\omega|^2)^{1/4} \sum_{n=0,1,2..} \frac{(z'_r/2)^{2n}}{\sqrt{2n!}} & \text{even states} \\ (1 - |\omega|^2)^{3/4} \sum_{n=0,1,2..} \frac{(z'_r/2)^{2n+1}}{\sqrt{(2n+1)!}} & \text{odd states} \end{cases} \quad (26a)$$

Therefore, we have

$$\langle \alpha_r, \varphi | \Psi(\omega) \rangle = (1 - |\omega|^2)^{1/4} \sum_{n=0,1,2..} (z'_r/2)^{2n} \left[\frac{1}{\sqrt{2n!}} + (1 - |\omega|^2)^{1/2} \frac{(z'_r/2)}{\sqrt{(2n+1)!}} \right] \quad (27)$$

We are now in a position to apply the Minimal Group representation by projecting the coherent states of the triangle according to the metaplectic representation.

$$\langle \alpha_{C_3}, \varphi | \Psi(\omega) \rangle = \mathcal{N} (1 - |\omega|^2)^{1/4} \sum_{r=1}^3 \sum_{n=0,1,2..} (z'_r/2)^{2n} \left[\frac{1}{\sqrt{2n!}} + (1 - |\omega|^2)^{1/2} \frac{(z'_r/2)}{\sqrt{(2n+1)!}} \right]$$

where

$$\begin{aligned} \omega e^{i(\varphi - \alpha^*/2)} &\equiv z'_1 \\ \omega e^{i(\varphi - e^{-\frac{2\pi i}{3}} \alpha^*/2)} &\equiv z'_2 \\ \omega e^{i(\varphi - e^{\frac{2\pi i}{3}} \alpha^*/2)} &\equiv z'_3 \end{aligned}$$

The square of the wave function (probability) takes the following form

$$\begin{aligned} |\langle \alpha_{C_3}, \varphi | \Psi(\omega) \rangle|^2 &= \mathcal{N}^2 (1 - |\omega|^2)^{1/2} \quad (28) \\ &\left\{ \sum_{r=s=1}^3 \left[\cosh(|z'_r/2|^2) + (1 - |\omega|^2) \sinh(|z'_r/2|^2) + (1 - |\omega|^2)^{1/2} \sum_{n=0,1,2..} \frac{(|z'_r|^2/4)^{2n} \operatorname{Re} z'_r}{\sqrt{(2n)!(2n+1)!}} \right] + \right. \\ &+ \sum_{r \neq s=1}^3 2 \left[\cosh\left(\frac{z'_r z'_s{}^* + z'_s z'_r{}^*}{4}\right) + (1 - |\omega|^2) \sinh\left(\frac{z'_r z'_s{}^* + z'_s z'_r{}^*}{4}\right) \right] \cosh\left(\frac{z'_r z'_s{}^* - z'_s z'_r{}^*}{4}\right) + \\ &\left. + (1 - |\omega|^2)^{1/2} \sum_{n=0,1,2..} \frac{(z'_r z'_s{}^*/4)^{2n} (z'_r + z'_s{}^*)}{\sqrt{(2n)!(2n+1)!}} \right\} \end{aligned}$$

We can see the projection in the even n sector $s = 1/4$

$$\begin{aligned}
|\langle \alpha_{C_3}, \varphi | \Psi_{1/4}(\omega) \rangle|^2 &= \mathcal{N}^2 (1 - |\omega|^2)^{1/2} \sum_{r=s=1}^3 \left[\sum_{n=0,1,2..} \frac{(|z'_r/2|^2)^{2n}}{2n!} \right] \\
&\quad + \sum_{r \neq s=1}^3 \sum_{n=0,1,2..} \left[\frac{(z'_r z'_s^*/4)^{2n}}{2n!} + \frac{(z'_s z'_r^*/4)^{2n}}{2n!} \right] \\
&= \mathcal{N}^2 (1 - |\omega|^2)^{1/2} \sum_{r=s=1}^3 \cosh(|z'_r/2|^2) + \sum_{r \neq s=1}^3 2 \cosh\left(\frac{z'_r z'_s^* + z'_s z'_r^*}{4}\right) \cosh\left(\frac{z'_r z'_s^* - z'_s z'_r^*}{4}\right)
\end{aligned}$$

using the expressions Eqs (19)-(21) and Eqs (29)-(34) below we have:

$$\begin{aligned}
|\langle \alpha_{C_3}, \varphi | \Psi_{1/4}(\omega) \rangle|^2 &= \mathcal{N}^2 (1 - |\omega|^2)^{1/2} \\
&\left\{ \sum_{r=s=1}^3 \cosh(|z'_r/2|^2) + 2 \cosh\left(\frac{|\omega|^2 e^{\frac{\alpha_I}{2}} \cos(\frac{\sqrt{3}}{2} \alpha_I)}{2}\right) \cos\left(\frac{|\omega|^2 e^{\frac{\alpha_I}{2}} \sin(\frac{\sqrt{3}}{2} \alpha_I)}{2}\right) + \right. \\
&\quad 2 \cosh\left(\frac{|\omega|^2 e^{-\frac{1}{2} \alpha_{3I}} \cos(-\frac{\sqrt{3}}{2} \alpha_{3I})}{2}\right) \cos\left(\frac{|\omega|^2 e^{-\frac{1}{2} \alpha_{3I}} \cos(-\frac{\sqrt{3}}{2} \alpha_{3I})}{2}\right) + \\
&\quad \left. + 2 \cosh\left(\frac{|\omega|^2 e^{\frac{1}{2} \alpha_{2I}} \cos(\frac{\sqrt{3}}{2} \alpha_{2I})}{2}\right) \cos\left(\frac{|\omega|^2 e^{\frac{1}{2} \alpha_{2I}} \cos(\frac{\sqrt{3}}{2} \alpha_{2I})}{2}\right) \right\}
\end{aligned}$$

Similarly, we can see the projection in the odd n sector $s = 3/4$

$$\begin{aligned}
|\langle \alpha_{C_3}, \varphi | \Psi_{3/4}(\omega) \rangle|^2 &= \mathcal{N}^2 (1 - |\omega|^2)^{3/2} \sum_{r=s=1}^3 \left[\sum_{n=0,1,2..} \frac{(|z'_r/2|^2)^{2n+1}}{(2n+1)!} \right] \\
&\quad + \sum_{r \neq s=1}^3 \sum_{n=0,1,2..} \left[\frac{(z'_r z'_s^*/4)^{2n+1}}{(2n+1)!} + \frac{(z'_s z'_r^*/4)^{2n+1}}{(2n+1)!} \right] \\
&= \mathcal{N}^2 (1 - |\omega|^2) \sum_{r=s=1}^3 \sinh(|z'_r/2|^2) + \sum_{r \neq s=1}^3 2 \sinh\left(\frac{z'_r z'_s^* + z'_s z'_r^*}{4}\right) \cosh\left(\frac{z'_r z'_s^* - z'_s z'_r^*}{4}\right)
\end{aligned}$$

Consequently

$$\begin{aligned}
|\langle \alpha_{C_3}, \varphi | \Psi_{3/4}(\omega) \rangle|^2 &= \mathcal{N}^2 (1 - |\omega|^2)^{3/2} \\
&\left\{ \sum_{r=s=1}^3 \sinh(|z'_r/2|^2) + 2 \sinh\left(\frac{|\omega|^2 e^{\frac{\alpha_I}{2}} \cos(\frac{\sqrt{3}}{2} \alpha_I)}{2}\right) \cos\left(\frac{|\omega|^2 e^{\frac{\alpha_I}{2}} \sin(\frac{\sqrt{3}}{2} \alpha_I)}{2}\right) + \right. \\
&\quad + 2 \sinh\left(\frac{|\omega|^2 e^{-\frac{1}{2} \alpha_{3I}} \cos(-\frac{\sqrt{3}}{2} \alpha_{3I})}{2}\right) \cos\left(\frac{|\omega|^2 e^{-\frac{1}{2} \alpha_{3I}} \cos(-\frac{\sqrt{3}}{2} \alpha_{3I})}{2}\right) \\
&\quad \left. + 2 \sinh\left(\frac{|\omega|^2 e^{\frac{1}{2} \alpha_{2I}} \cos(\frac{\sqrt{3}}{2} \alpha_{2I})}{2}\right) \cos\left(\frac{|\omega|^2 e^{\frac{1}{2} \alpha_{2I}} \cos(\frac{\sqrt{3}}{2} \alpha_{2I})}{2}\right) \right\}
\end{aligned}$$

where the following expressions were also taken into account:

$$z'_2 z'_3{}^* + z'_3 z'_2{}^* = 2 |\omega|^2 e^{\frac{\text{Im } \alpha}{2}} \cos \left(\frac{\sqrt{3}}{2} \text{Im } \alpha \right) \quad (29)$$

$$z'_2 z'_3{}^* - z'_3 z'_2{}^* = -2i |\omega|^2 e^{\frac{\text{Im } \alpha}{2}} \sin \left(\frac{\sqrt{3}}{2} \text{Im } \alpha \right) \quad (30)$$

$$z'_1 z'_2{}^* + z'_2 z'_1{}^* = 2 |\omega|^2 e^{\frac{1}{4}(\text{Im } \alpha + \sqrt{3} \text{Re } \alpha)} \cos Z_{(+)}(\alpha) \quad (31)$$

$$z'_1 z'_2{}^* - z'_2 z'_1{}^* = -2i |\omega|^2 e^{\frac{1}{4}(\text{Im } \alpha + \sqrt{3} \text{Re } \alpha)} \sin Z_{(+)}(\alpha) \quad (32)$$

$$z'_3 z'_1{}^* + z'_1 z'_3{}^* = 2 |\omega|^2 e^{-\frac{1}{4}(\text{Im } \alpha - \sqrt{3} \text{Re } \alpha)} \cos Z_{(-)}(\alpha) \quad (33)$$

$$z'_3 z'_1{}^* - z'_1 z'_3{}^* = -2i |\omega|^2 e^{-\frac{1}{4}(\text{Im } \alpha - \sqrt{3} \text{Re } \alpha)} \sin Z_{(-)}(\alpha) \quad (34)$$

Here we have defined:

$$Z_{(\pm)}(\alpha) \equiv \frac{\sqrt{3}}{4} \left(\text{Im } \alpha \pm \sqrt{3} \text{Re } \alpha \right)$$

VI. TOPOLOGICAL SEPARATION CONDITIONS OF THE EVEN AND ODD SECTORS $S = 1/4$ AND $S = 3/4$

It is evident from the application of the Metaplectic Group action, that the expression of the probability appears as the sum of even and odd probabilities (without mixed terms) if:

$$z'_r = -z'_s{}^* \quad \text{for} \quad r \neq s$$

and

$$\text{Re } z'_r = 0 \quad \text{for} \quad r = s.$$

(i) The case $\text{Re } z'_r = 0$

Omitting the subscript r in the final formula and decomposing α_r and ω in the real and imaginary parts we obtain

$$\begin{aligned} z'_r &= \omega e^{i(\varphi - \alpha_r^*/2)} \\ &= e^{-\alpha_{rI}/2} \{ [\omega_R \cos(\varphi - \alpha_{rR}/2) - \omega_I \sin(\varphi - \alpha_{rR}/2)] + \\ &\quad + i [\omega_I \cos(\varphi - \alpha_{rR}/2) + \omega_R \sin(\varphi - \alpha_{rR}/2)] \} \end{aligned}$$

Consequently,

$$\begin{aligned}\operatorname{Re} z'_r = 0 &\implies \omega_R = \omega_I \tan(\varphi - \alpha_{rR}/2) \\ z'_r &= 2e^{-\alpha_{rI}/2} i \omega_I \sin(\varphi - \alpha_{rR}/2)\end{aligned}$$

This case is analog to the purity condition in the circle [8].

(ii) The case $z'_r = -z'_s^*$

Knowing that

$$\begin{aligned}z'_s^* &= \sigma^* e^{-i(\varphi' - \alpha_s/2)} \\ &- \alpha_{sI}/2 \{ [\sigma_R \cos(\varphi' - \alpha_{sR}/2) - \sigma_I \sin(\varphi' - \alpha_{sR}/2)] - \\ &- i [\sigma_I \cos(\varphi' - \alpha_{sR}/2) + \sigma_R \sin(\varphi' - \alpha_{sR}/2)] \}\end{aligned}$$

We have the expressions:

$$\begin{aligned}\omega e^{i(\varphi - \alpha_r^*/2)} &= -\sigma^* e^{-i(\varphi' - \alpha_s/2)} \\ \frac{\omega \sigma}{|\sigma|^2} &= -e^{-i[(\varphi' + \varphi) - (\alpha_s + \alpha_r^*)/2]}\end{aligned}$$

(where we see that the functions on the disk namely ω and σ are linked exponentially with the $\varphi', \varphi, \alpha_s, \alpha_r^*$ operating as control parameters).or the following ones :

$$e^{-\alpha_{rI}/2} [\omega_R \cos(\varphi - \alpha_{rR}/2) - \omega_I \sin(\varphi - \alpha_{rR}/2)] = -e^{-\alpha_{sI}/2} [\sigma_R \cos(\varphi' - \alpha_{sR}/2) - \sigma_I \sin(\varphi' - \alpha_{sR}/2)]$$

and

$$e^{-\alpha_{rI}/2} [\omega_I \cos(\varphi - \alpha_{rR}/2) + \omega_R \sin(\varphi - \alpha_{rR}/2)] = e^{-\alpha_{sI}/2} [\sigma_I \cos(\varphi' - \alpha_{sR}/2) + \sigma_R \sin(\varphi' - \alpha_{sR}/2)]$$

VII. GENERALIZATION OF THE BARGMANN REPRESENTATION AND THE METAPLECTIC SYMMETRY

To this end, we start from the case of the standard Bargmann representation of the basic states of the Mp(2) in the oscillator representation

$$\langle n | | \Psi(\omega(z)) \rangle \left\{ \begin{array}{l} (1 - |\omega(z)|^2)^{1/4} \sum_{n=0,1,2..} \frac{(\omega(z)/2)^{2n}}{\sqrt{2n!}} \quad \text{even states} \\ (1 - |\omega(z)|^2)^{3/4} \sum_{n=0,1,2..} \frac{(\omega(z)/2)^{2n+1}}{\sqrt{(2n+1)!}} \quad \text{odd states} \end{array} \right. \quad (35a)$$

where the function $\omega(z)$ is the conformal mapping from the equilateral triangle to the unit disk according to the Schwartz-Christoffel type transformation, namely,

$$\omega(z) = \frac{2^{11/6} \cos(\pi/12) (1 - cn(\xi, m)) (1 - \tan(\pi/12) cn(\xi, m))}{2 \cdot 3^{1/4} sn(\xi, m) dn(\xi, m) + (1 - cn(\xi, m))^2}$$

with

$$\xi = \frac{z (\Gamma(1/3))^3}{2^{1/3} 3^{1/4} \pi}, \quad m = \sin(\pi/12)^2$$

The mapping (for discrete series) is represented graphically in the Figures (7) and (8). According to the expressions Eqs (35a) the expansions of the first terms of the even and odd states are represented in the Figure (9) where an asymmetry can be seen for the n multiples of 3 (sides of the triangle).

VIII. REMARKS AND CONCLUSIONS

In this paper we have computed and analyzed the geometrical and topological changes in quantum physics within the new framework of our recent work Ref [8] on Classicalization. Thus, the results of our paper here are twofold : **Topology, geometry and Classicalization and the relationship between them**. In Section I we summarized the main results of the study performed here and we do not explicitate them here again. In this Section we just briefly highlight main concluding remarks in a synthetic way. We consider various types of states on the simplest polygon: states with triangle topology as solution of the Schrodinger equation, eigenstates of a lowering operator and coset coherent states.

We highlight here the following conclusions of this paper:

(1) From the point of view of the metaplectic group and the classification, the application of the Minimal Group Representation (MGR) would be possible on the states of Section I if the ladder operators A_n and A_{-n} are related to those of the oscillator a and a^+

(2) For the coherent state case in Section I, the application of the MGR can be viewed in the same way as (1) but considering an eigenstate of the operator A_{-1} , or a more general case, as an eigenstate of A_{-n} .

(3) These 2D states described in Sections I and II are edge states geometrically dual to the quantum states within the boundary of the triangle (ref. [15]): there is interplay between states at the edge and the states inside the triangular boundary (Figs. 3-6).

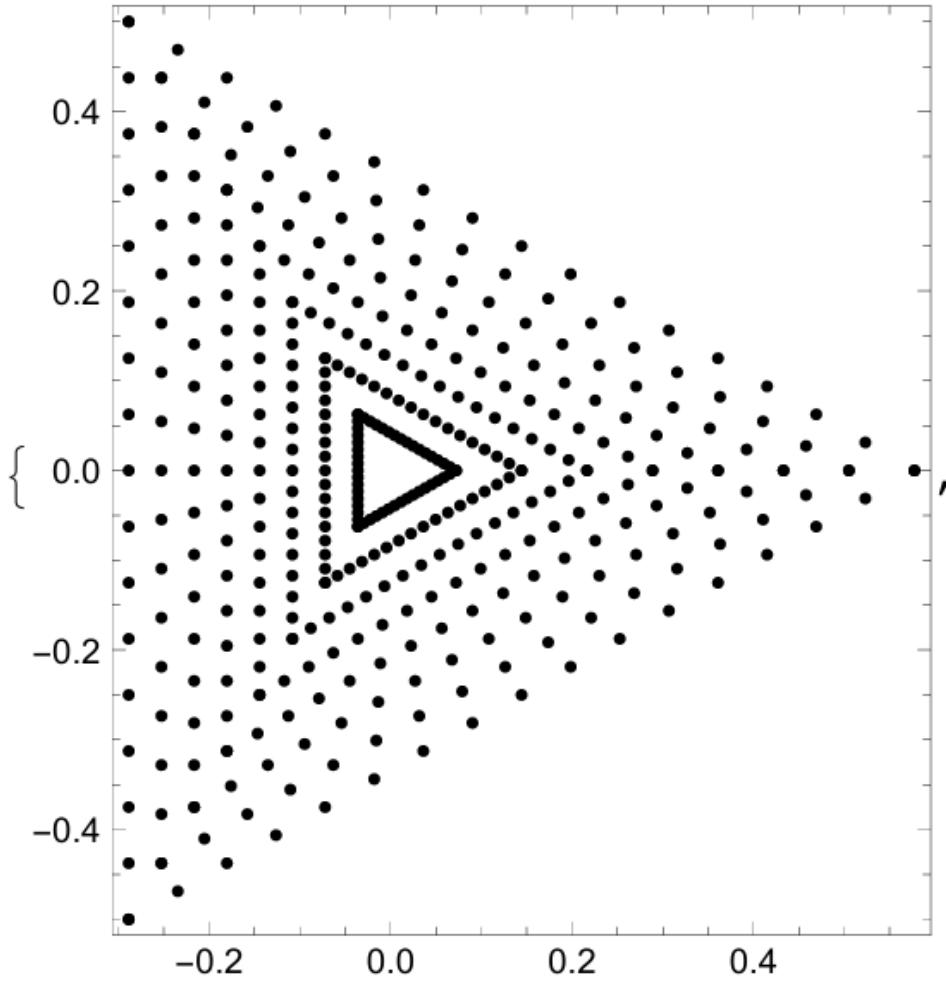


FIG. 7: Discrete series in the triangular region to be conformally mapped to the disk, geometric basis of Bargmann's representation of quantum states (coherent states in particular).

(4) From Section III, the coherent states in the triangle are generated by applying the group D_3 to the coset coherent states of the circle as a fiducial vector (e.g., a polygon with ∞ sides).

(5) The justification for the proposal in point 4) is easy to see by applying the cyclic subgroup C_n of D_n to the fiducial (coset circle coherent states): as the number of sides tends to infinity, the elements of C_n tend to identity.

(6) The application of MGR in the case of D_3 (D_n) coherent state, reveals to us the quantum structure underlying each of the sides of the triangle (polygon).

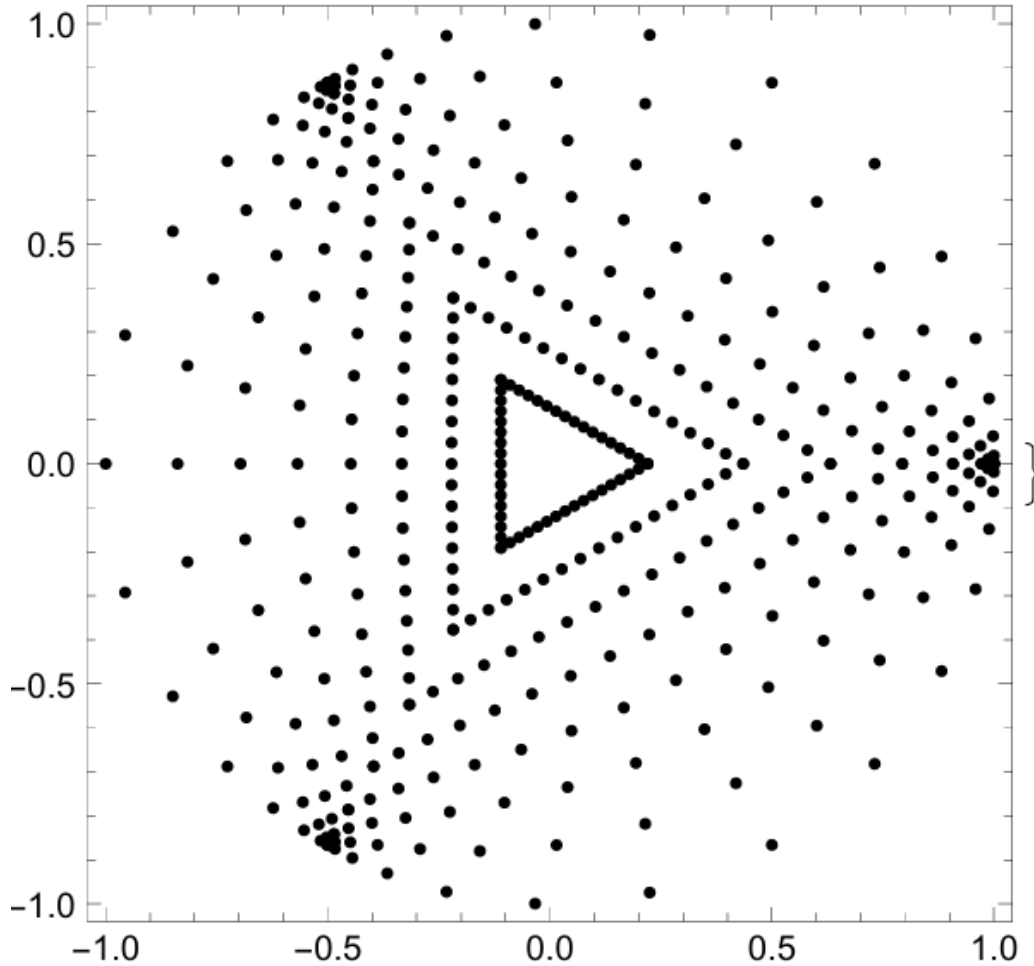


FIG. 8: Discrete series of the triangular region conformally mapped to the disk. We can see the accumulation of discretization points in the position of the vertices (fixed points of the transformation) of the conformally mapped triangle.

(7) The calculation of the norm (probability) shows clear interaction/interference between the sides and between the even and odd sectors of the Hilbert space.

(8) The application of MGR allows topological isolation between the projected sectors (even and odd) through the conditions of Section VI. It can be seen that the topological effect is of a quantum nature and vice versa.

(9) From the item (8) above we can see that these topological isolation effects do not disappear at the macroscopic level (e.g. they are independent of the space-time parameters of the physical system)

(10) A generalization of the Bargmann Representation and the Metaplectic Symmetry is given where the analytical function is the conformal transformation of the equilateral triangle in the unit disk.

(11) From (10), the mapping (for discrete series), represented graphically in the Figures (7) and (8),. and due to Eqs (35a) an asymmetry can be seen for the n multiples of 3 (sides of the triangle).

(12) **Outlook and Implications:** In general, the results here show too from the metaplectic MGR that quantum states in geometries with angles and vertices classicalize more than in geometries without them. These properties have consequences for the better geometries should be chosen for quantum computation devices and quantum information transmission.

The results of this paper on theoretical and conceptual aspects of quantum theory and its classicalization can have impact and applications in different branches of physics and other disciplines.

For instance:

(i) By choosing a type of geometry- topology of the states, one can obtain stronger or lower classicalization.

(ii) By using or avoiding coincident or orthogonal states, one can allows or avoid that entanglement be decreasing, broken or vanishing.

(iii) By choosing Antipodal or Non Antipodal Entanglement (regulating the phase control parameter ρ be equal to π or 0 respectively), Entanglement can be lower, minimal or not.

(iv) Combination of possibilities (i)-(ii)-(iii) could yield more effects.

IX. ACKNOWLEDGEMENTS

D.J.C.-L. acknowledges the Special Astrophysical Observatory of the Russian Academy of Sciences and CONICET of Argentine for Institutional and financial support. This work was carried out within the framework of a state assignment for SAO-RAS, approved by the Ministry of Science and Higher Education of the Russian Federation.

X. APPENDIX: COSET COHERENT STATES ALTERNATIVE NORMALIZATION

Here we give an alternative normalization to the coherent states of Section IV.

$$\begin{aligned}
|\alpha_{C_3}, \varphi\rangle &= \mathcal{N} \left(\sum_{r=1}^3 |\alpha_r, \varphi\rangle \right) \\
&= \mathcal{N} (|\alpha_1, \varphi\rangle + |\alpha_2, \varphi\rangle + |\alpha_3, \varphi\rangle) \\
&= \frac{\mathcal{N}}{\sqrt{2\pi}} (S(\alpha_1, \varphi) |\varphi - \alpha_1/2\rangle + S(\alpha_2, \varphi) |\varphi - \alpha_2/2\rangle + S(\alpha_3, \varphi) |\varphi - \alpha_3/2\rangle)
\end{aligned} \tag{36}$$

from (16)

$$|\alpha_{C_3}, \varphi\rangle = \frac{\mathcal{N}}{\sqrt{2\pi}} \left(S(\alpha, \varphi) |\varphi - \alpha/2\rangle + S\left(e^{\frac{2\pi i}{3}} \alpha, \varphi\right) \left| \varphi - e^{\frac{2\pi i}{3}} \alpha/2 \right\rangle + S\left(e^{-\frac{2\pi i}{3}} \alpha, \varphi\right) \left| \varphi - e^{-\frac{2\pi i}{3}} \alpha/2 \right\rangle \right)$$

the overlap can be easily computed

$$\begin{aligned}
\langle \alpha_{C_3}, \varphi | \alpha_{C_3}, \varphi \rangle &= \left(\frac{\mathcal{N}}{\sqrt{2\pi}} \right)^2 \sum_{r=1}^3 \left[\frac{S(\alpha_r^*, \varphi) S(\alpha_r, \varphi)}{1 - e^{\text{Im} \alpha_r}} + \right. \\
&\quad \left. + \sum_{s \neq r=1}^3 \left(\frac{S(\alpha_s^*, \varphi) S(\alpha_r, \varphi)}{1 - e^{i(\alpha_r - \alpha_s^*)/2}} + \frac{S(\alpha_r^*, \varphi) S(\alpha_s, \varphi)}{1 - e^{i(\alpha_s - \alpha_r^*)/2}} \right) \right] \\
\mathcal{N}^2 &= \frac{2\pi}{\sum_{r=1}^3 \left[\frac{S(\alpha_r^*, \varphi) S(\alpha_r, \varphi)}{1 - e^{\text{Im} \alpha_r}} + \sum_{s \neq r=1}^3 \left(\frac{S(\alpha_s^*, \varphi) S(\alpha_r, \varphi)}{1 - e^{i(\alpha_r - \alpha_s^*)/2}} + \frac{S(\alpha_r^*, \varphi) S(\alpha_s, \varphi)}{1 - e^{i(\alpha_s - \alpha_r^*)/2}} \right) \right]}
\end{aligned} \tag{37}$$

XI. AUTHOR DECLARATIONS

A. Conflict of Interest

The authors have no conflicts to disclose.

B. Author Contributions

Diego J. Cirilo-Lombardo: Conceptualization (equal); Data curation (equal); Formal analysis (equal); Investigation (equal); Methodology (equal); Project administration (equal); Resources (equal); Software (equal); Supervision (equal); Validation (equal); Visualization

(equal); Writing – original draft (equal); Writing – review & editing (equal). Norma G. Sanchez: Conceptualization (equal); Data curation (equal); Formal analysis (equal); Investigation (equal); Methodology (equal); Project administration (equal); Resources (equal); Software (equal); Supervision (equal); Validation (equal); Visualization (equal); Writing – original draft (equal); Writing – review & editing (equal).

XII. DATA AVAILABILITY

The data that support the findings of this study are available within the article.

- [1] Ortwin Hess *From Quantum physics to Quantum science*, APL Quantum 1, 010401 (2024); <https://doi.org/10.1063/5.0202749>

- [2] Alain Aspect, John F. Clauser and Anton Zeilinger, Nobel Prize in Physics 2022, "for experiments with entangled photons, ... and pioneering quantum information science" <https://www.nobelprize.org/uploads/2023/10/advanced-physicsprize2022-4.pdf> and Refs therein.

- [3] John J. Hopfield and Geoffrey E. Hinton, Nobel Prize in Physics 2024, "for foundational discoveries and inventions that enable machine learning with artificial neural networks" <https://www.nobelprize.org/uploads/2024/10/advanced-physicsprize2024-2.pdf> and Refs therein.

- [4] J. L. Mac Loughlin, N. G. Sanchez, "Photography as a New Conceptual Quantum Information System" <https://www.researchgate.net/publication/375745724> <https://www.bibsonomy.org/bibtex/7a77b52e38f27089f47229b1193dc005>

- [5] J. L. Mac Loughlin, N. G. Sanchez, "Photography as a Quantum Information System and the Nobel Prize in Physics 2025 : A Synthesis",

<https://www.researchgate.net/publication/396743961>

https://chalonge-devega.fr/Photography_Q-MacroscopicSystem_JLMacL_NGS_EN.pdf

[6] The International Year of Quantum Science and Technology (IYQ-2025),

See for example: <https://quantum2025.org/>

https : //qt.eu/news/2024/2024 – 06 – 07UN – declares – 2025 – international – year – of – quantum – science – and – technology

[7] D. J. Cirilo-Lombardo, N. G. Sanchez, Universe 2024, 10(1), 22;

<https://doi.org/10.3390/universe10010022>

[8] D. J. Cirilo-Lombardo, N. G. Sanchez, APL Quantum 2, 016104 (2025).

<https://doi.org/10.1063/5.0247698>

<https://pubs.aip.org/aip/apq/article/2/1/016104/3329660/Classical-ontological-dual-states-in-quantum>

[9] D. J. Cirilo-Lombardo, N. G. Sanchez,, IJGMMP, online ready (2025)

<https://doi.org/10.1142/S0219887826500490>

[10] N. G. Sanchez, Phys. Rev. D 104, 123517 (2021).

<https://doi.org/10.1103/physrevd.104.123517>

[11] N. G. Sanchez, Phys. Rev. D 107, 126018 (2023).

<https://doi.org/10.1103/physrevd.107.126018>

[12] N. G. Sanchez, Int. J. Mod Phys D28, 1950055 (2019).

<https://doi.org/10.1142/S021827181950055X>

[13] N. G. Sanchez, Int. J. Mod Phys A34, 1950155 (2019).

<https://doi.org/10.1142/S0217751X19501550>

- [14] N. G. Sanchez, *Gravit. Cosmol.* 25, 91-102 (2019).
<https://doi.org/10.1134/S0202289319020142>
- [15] S. M. Blinder, *J. Math. Phys.* 26 (11), (1985)
- [16] Castaños, O., Lopez-Peña, R. & Man'ko, V.I. Crystallized Schrödinger cat states. *J Russ Laser Res* 16, 477–525 (1995)

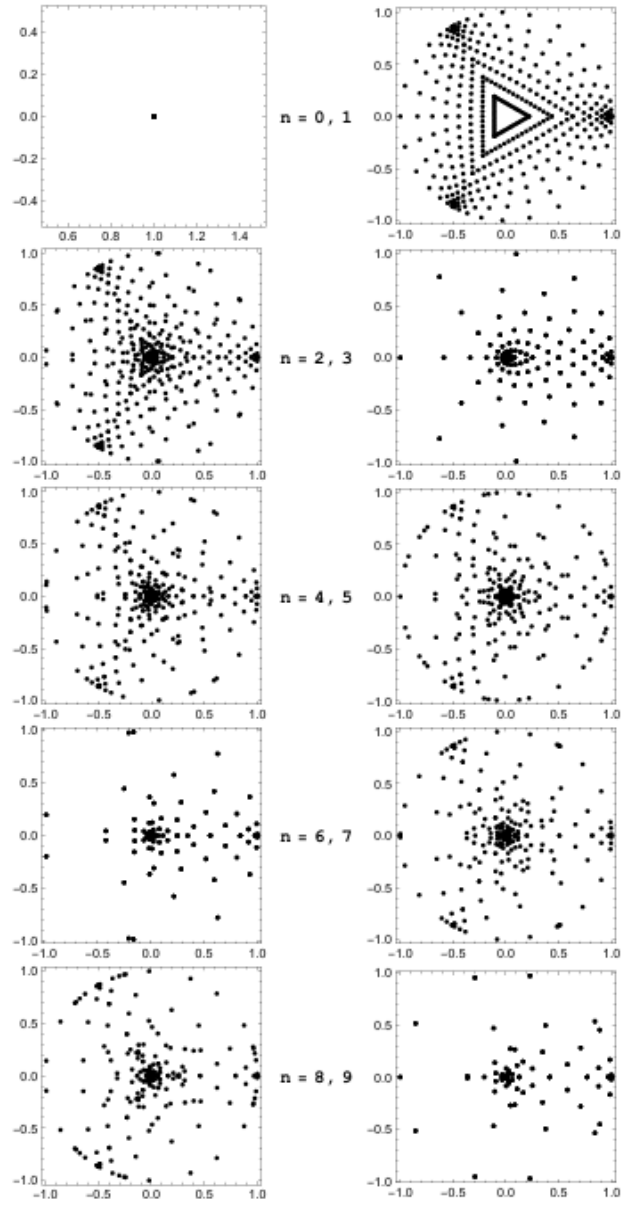


FIG. 9: Expansion of the basic coherent states of $Mp(2)$ (even in the left column and odd in the right) according to the Bargmann representation where the analytical function is the conformal transformation of the equilateral triangle in the unit disk.